Structure and Properties of Strain-Induced Crystallization Rubber–Clay Nanocomposites by Co-coagulating the Rubber Latex and Clay Aqueous Suspension

Yiqing Wang,[1] Huifeng Zhang,[1] Youping Wu,[1] Jun Yang,[2] Liqun Zhang[1,2]

[1]*Key Laboratory for Nano-materials, Ministry of Educational, Beijing 100029, China*
[2]*Key Laboratory of Beijing City on Preparation and Processing of Novel Polymer Materials, Beijing University of Chemical Technology, Beijing 100029, China*

Received 20 May 2003; accepted 13 August 2004
DOI 10.1002/app.21408
Published online in Wiley InterScience (www.interscience.wiley.com).

ABSTRACT: Natural rubber (NR)–clay (clay is montmorillonite) and chloroprene rubber (CR)–clay nanocomposites were prepared by co-coagulating the rubber latex and clay aqueous suspension. Transmission electron microscopy showed that the layers of clay were dispersed in the NR matrix at a nano level, and the aspect ratio (width/thickness) of the platelet inclusions was reduced and clay layers aligned more orderly during the compounding operation on an open mill. However, X-ray diffraction indicated that there were some nonexfoliated clay layers in the NR matrix. Stress–strain curves showed that the moduli of NR were significantly improved with the increase of the amount of clay. At the same time, the clay layers inhibited the crystallization of NR on stretch, especially clay content of more than 10 phr. Compared with the carbon-black-filled NR composites, NR–clay nanocomposites exhibited high hardness, high modulus, high tear strength, and excellent antiaging and gas barrier properties. Similar to NR–clay nanocomposites, CR–clay nanocomposites also exhibited high hardness, high modulus, and high tear strength. © 2005 Wiley Periodicals, Inc. J Appl Polym Sci 96: 318–323, 2005

Key words: clay; strain-induced crystallization rubber; nanocomposites; structure; mechanical properties; gas permeability

INTRODUCTION

Polymer–clay nanocomposites, especially plastic matrices, have attracted much attention recently, and these nanocomposites exhibit outstanding mechanical properties, low gas permeability, and excellent fire retardant properties[1–6]. But there are only a few studies on rubber–clay nanocomposites. Synthesis of rubber–clay nanocomposites has typically involved rubber melt or solution intercalation of organclay, which has organic ammonium salts, or protonated amino-terminated polybutadiene/poly(butadiene-*co*-arylonitrile) in the interlayer space[7–10]. A new approach for rubber matrices introduced in a patent[11] by the authors of this article involves mixing the rubber latex and the clay aqueous suspension and cocoagulating by adding electrolyte, which is simpler and cheaper than the methods using organic clay. In our previous work, morphology and mechanical properties of noncrystallizing rubber such as styrene butadiene rubber–, carboxylated acrylonitrile butadiene–, and nitrile rubber–clay nanocomposites are investigated[12–15]. Since natural rubber (NR) and chloroprene rubber (CR) are strain-induced crystallization rubbers and possess high strength without reinforcement, it is interesting to investigate the properties of NR–clay and CR–clay nanocomposites. In this paper, the effects of the amounts of clay on mechanical properties, gas permeability, and air-oven aging properties of NR–clay or CR–clay nanocomposites are studied in detail.

Correspondence to: L-Q. Zhang (zhangliqunghp@yahoo.com).

Contract grant sponsor: National Natural Science Foundation of China; contract grant number: 05173003; contract grant sponsor: Beijing New Star Plan Project; contract grant number: H010410010112; contract grant sponsor: Key Project of Beijing Natural Science Foundation; contract grant number: 2031001; contract grant sponsor: National Tenth-five Program; contract grant number: 2001BA310A12.

EXPERIMENTAL PROCEDURES

Materials

The clay (Na-montmorillonite), with a cationic exchange capacity of 93 meq/100 g, is from Liufangzi Clay Factory (Jilin, China). NR latex is from Beijing Latex Products Factory (China). CR latex is from Shanxi Latex Factory (China).

Preparation of rubber-clay nanocomposites

The clay aqueous suspension, the rubber latex, and the interfacial agent ($C_4H_9N^+(CH_2CH_2OH)_3Br^-$, 0.1 mol/

TABLE I
Recipe of NR Matrix Composites (phr)

NR	100
Filler	Variable
Zinc oxide	5.0
Stearic acid	2.0
Dibenzothiazole disulfide (DM)	0.5
Diphenyl guanidine (D)	0.5
Tetramethyl thiuram disulfide (TMTD)	0.2
Sulfur (S)	2.0
N-isopropyl-*N*′-phenyl-*p*-phenylene diamine (Antioxidant 4010NA)	1.0

100 g) were mixed and vigorously stirred for a given period of time. After that, the mixture was coagulated in the electrolyte solution (2% dilute sulfuric acid), washed with water until its pH was about 7, and dried in an oven for 20 h at 60°C. Then the rubber–clay nanocompound was obtained.

The vulcanizing ingredients and other additives, shown in recipes in Table I and Table II for NR and CR, respectively, were mixed into the nanocompound with a 6-inch two-roll mill; then the compound was vulcanized in a standard mold at 150°C for optimal cure time (t_{90}), which was determined by a rheometer (Beijing Huan Feng Mechanical Factory). The vulcanizates were referred to as rubber–clay nanocomposites.

Vulcanizates filled with carbon black (N330), silica, and clay were prepared by directly mixing the filler into rubber. The additives and the curing condition were the same as for the rubber–clay nanocomposites.

Characterization

Transmission electron microscopy (TEM) micrographs were taken from ultrathin sections with an H-800 TEM, using an acceleration voltage of 200 Kv. XRD analyses were carried out on Rigaku RINT using CuKα radiation, a 0.02°C step size, and 5.0, 2 θ/min. Shore A hardness was measured according to ISO 48–1994. Tensile tests were performed on dumbbell-shape specimens according to ISO 37–1994. Tear strength was carried out according to ISO 34–1 1994. Five samples were tested and the average of the values was taken.

TABLE II
Recipe of CR Matrix Composites (phr)

CR	100
Filler	0, 5, 10, 20, 30
Zinc oxide	4.0
Magnesium oxide	5.0
Antioxidant 4010NA	1.0

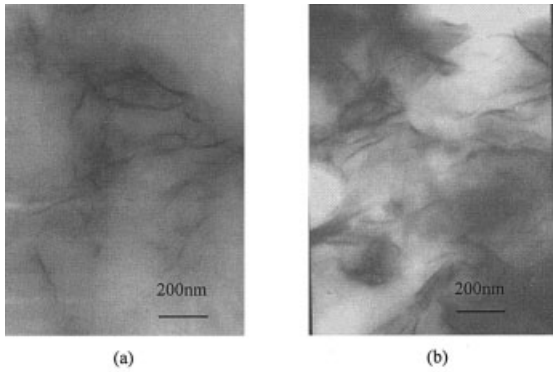

Figure 1 TEM micrographs of NR–clay nanocompounds. NR–clay (w/w): (a) 100/10; (b) 100/20.

Air aging of the samples was performed by a 401-A air aging oven (Shanghai Instrument Factory) according to ISO-188–1998.

Abrasion resistance (Akron machine) was carried out according to GB/T 1689–1998.

The permeation experiment of nitrogen was carried out with a gas-permeability-measuring apparatus. The pressure on one face of the sheet (about 1 mm thickness and 8 cm diameter) was kept at 0.57 MPa and the other face at zero pressure initially, and the nitrogen permeated through the sheet. The rate of transmission of nitrogen at 40°C was obtained by gas chromatography and the nitrogen permeability was calculated from it.

RESULTS AND DISCUSSION

Morphology

TEM micrographs of the NR–clay nanocompounds containing 10 and 20 phr clay are shown in Figure 1. The dark lines in Figure 1a and b are the intersections of the clay layers. As seen in Figure 1a and b, clay layers are entangled, folded, disordered, and homogeneously dispersed in the NR matrix, and the thickness of most clay layers is about 10 nm and the width about 200–400 nm. Moreover, there are some exfoliated individual clay layers.

TEM micrographs of the NR–clay nanocomposites (namely vulcanizates) containing 10 and 20 phr clay are shown in Figure 2. Compared with Figure 1, it is shown that the aspect ratio (width/thickness) of clay layers in Figure 2 decreases and the orientation of clay layers improves considerably, which is attributed to the high shear force in the nip region of open-mill rolls during mixing vulcanizing agents into the NR–clay nanocompound.

The XRD patterns of MMT and the NR–clay nanocomposites with different clay loading amounts are presented in Figure 3, where diffraction peaks correspond to the (001) plane reflections of the clay. From

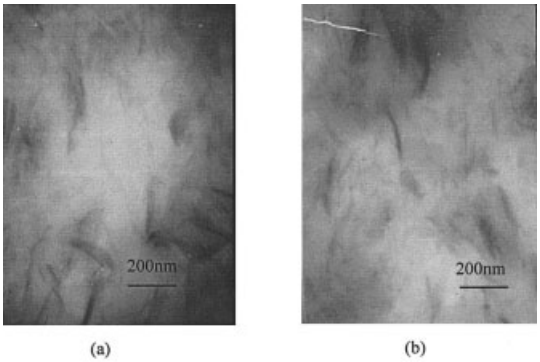

Figure 2 TEM micrographs of NR–clay nanocomposites. NR–clay (w/w): (a) 100/10; (b) 100/20.

Figure 3, the position of peaks of the NR–clay nanocomposites is almost the same as that of MMT, indicating that rubber molecules do not intercalate into the intergallery of MMT. The intensity of peak increases with the growth of the clay content, suggesting the increase of the amount of nonexfoliated layers with the increase of clay amount. The nonexfoliated clay layers are evident in Figures 1 and 2.

According to the results of TEM micrographs and XRD patterns, the schematic of the structure of NR–clay nanocomposites prepared by cocoagulating the rubber latex and clay aqueous suspension is shown in Figure 4. Rubber macromolecules do not intercalate the gallery of clay, but separate the pristine clay into 10- to 20-nm-thick layers and even individual layers. The above structure is different from the intercalated or exfoliated or the combination of intercalated and exfoliated clay–polymer nanocomposites in the open literature[16].

Properties of NR–clay nanocomposites

Stress–strain curves of NR–clay nanocomposites with various clay contents are shown in Figure 5. The unfilled NR demonstrates a typical strain-induced crystallization behavior. In the lower strain region, the modulus is low and slowly increases with the increase in strain; when the strain is larger than about 450%, the stress increases sharply due to the occurrence and subsequent rapid development of tensile crystallization. For NR–clay nanocomposites, the initial part of stress–strain is higher than that of gum NR. The magnitude of improvement rises with the increase of clay loading. Correspondingly, due to the hindrance of clay to the tensile crystallization, the phenomenon of sharp increase of stress caused by tensile crystallization gradually disappears.

The tensile strength of NR–clay nanocomposites originates from two aspects, the strain-induced crystallization and the reinforcement of nanodispersed clay layers. The NR–clay nanocomposite containing 5

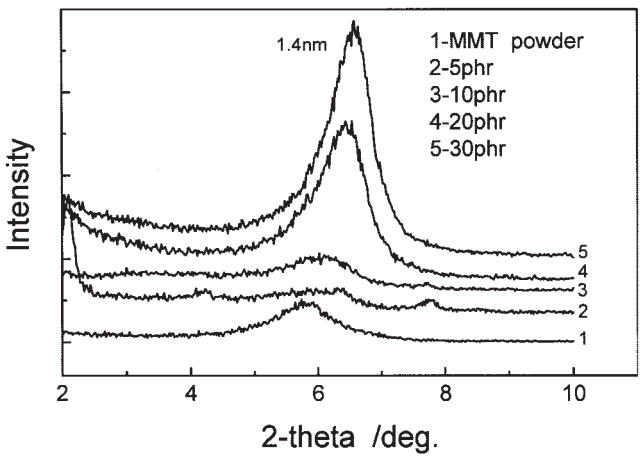

Figure 3 X-ray diffraction patterns of NR–clay nanocomposites.

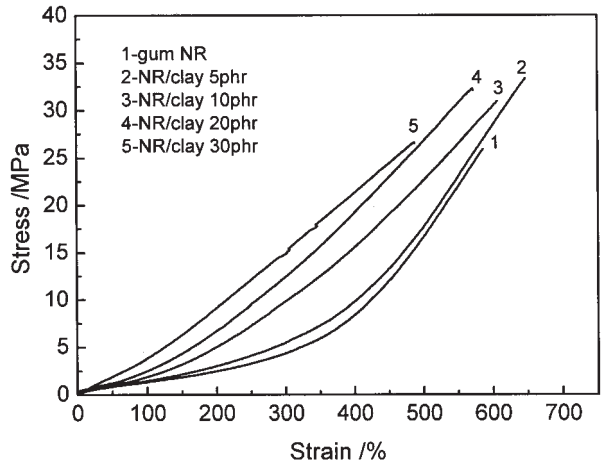

Figure 5 The curves of stress–strain of NR–clay nanocomposites with different clay amount.

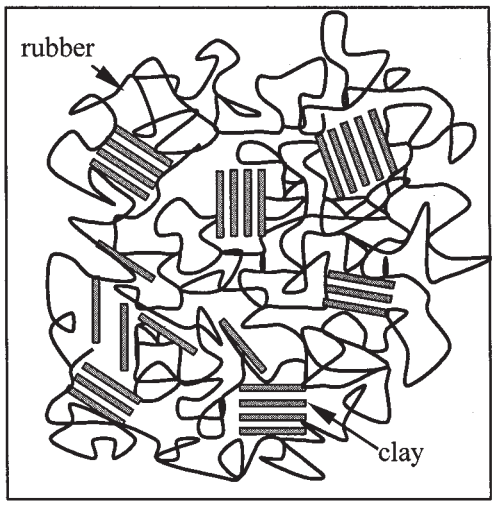

Figure 4 The schematic of the rubber–clay nanocomposites.

TABLE III
The Mechanical and Abrasion Properties of NR–Clay Composites

	Nanocomposites						Conventional composites				
Clay content, phr	0	5	10	20	30	40	5	10	20	30	40
Hardness, shore A	39	42	45	54	62	68	38	37	39	38	37
300% Modulus, MPa	2.0	4.5	6.2	12.3	15.9	17.2	2.1	2.2	2.0	2.2	2.4
Tensile strength, MPa	26.9	34	33.8	29.2	26.3	25.3	16.6	15.6	17.1	18.1	17.1
Tear strength, KN/m	26.6	36.4	43.3	44.1	44.8	45.2	26.4	22.9	22.8	23.3	21.4
Akron abrasion, cm^3/1.61 km	1.279	0.803	0.61	0.386	0.292	0.368	1.314	1.082	1.041	2.017	2.014

phr clay exhibits evident strain-induced crystallization, and its tensile strength is higher than that of gum NR due to the reinforcement of clay. When the amount of clay is more than 10 phr, the strain-induced crystallization is hindered, and the tensile strength results from the reinforcement of clay layers. Compared with the NR–clay nanocomposite containing 20 phr clay, the tensile strength of the NR–clay nanocomposite containing 30 phr decreases, which should be attributed to the increase of amount of nonexfoliated clay layers, as shown in Figure 3. However, the tensile strength of the nonacomposites based on a non-strain-induced rubber will gradually increase with the increase of clay content within 40 phr[13].

The mechanical and abrasion properties of NR–clay nanocomposites are presented in Table III. Conventional NR–clay composites are compared to NR–clay nanocomposites containing the equivalent amount

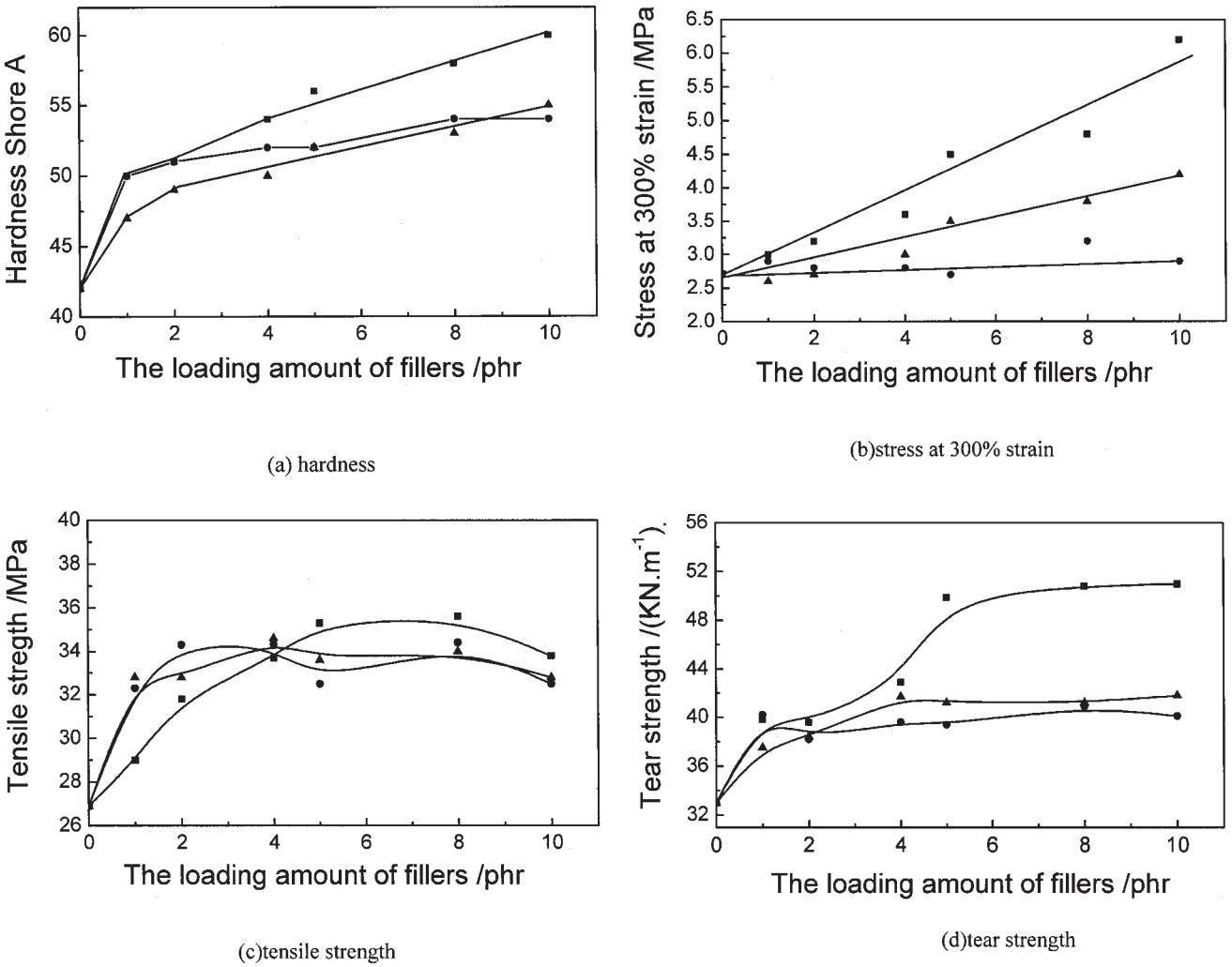

Figure 6 Mechanical properties of NR with different fillers: (a) hardness; (b) stress at 300% strain; (c) tensile strength; (d) tear strength. ■, nanocomposites; ▲, carbon black/NR composites; ●, silica/NR composites.

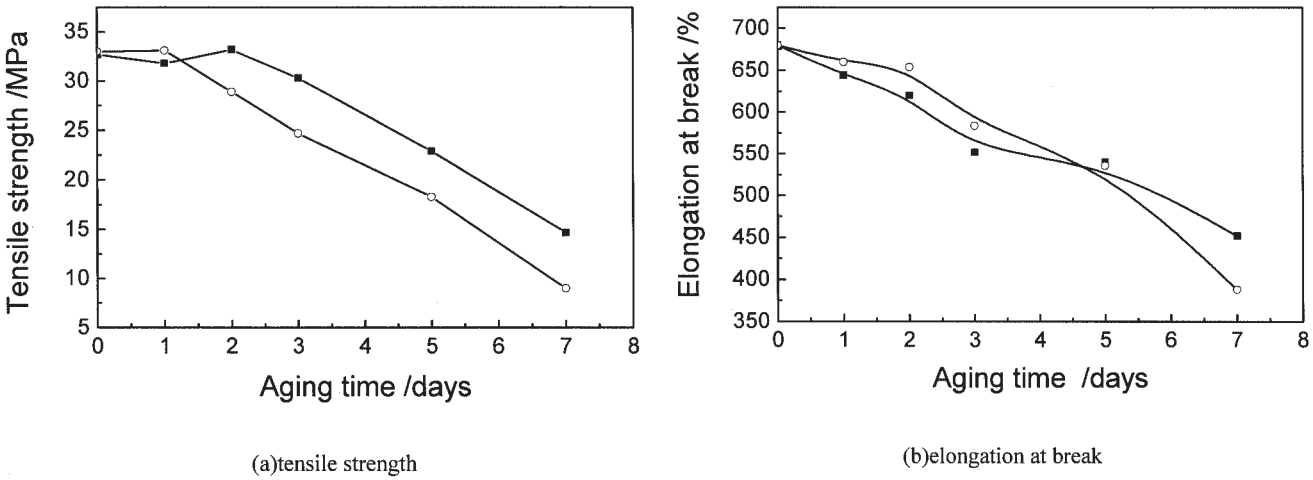

Figure 7 Aging properties of NR–clay nanocomposites and carbon black/NR composites: (a) tensile strength; (b) elongation at break. ■, nanocomposites; ○, carbon black/NR composites.

clay. As seen in Table III, the NR–clay nanocomposites exhibit higher hardness, modulus, tear strength, and tensile strength and better abrasion properties in contrast to conventional composites. The tear strength and Akron abrasion of nanocomposites with 10 phr clay is 43.3 KN/m and 0.61 cm^3/1.61 km, an increase 62.8 and 52.3%, respectively, compared with the gum NR vulcanizate. The NR–clay nanocomposite with 10 phr clay has the best overall properties.

Since carbon black and silica are the most common reinforcing fillers for rubber, the mechanical properties of NR–clay nanocomposites with different amounts of clay (less than 10 phr) were compared to those of NR filled with equivalent amounts of carbon black or silica, and the results are presented in Figure 6. The hardness, modulus, tensile, and tear strength increase with the amount of filler increasing, and NR–clay nanocomposites have the highest modulus and tear strength. The results should be assigned to the large aspect ratio of clay layers since carbon black and silica are nanoscale spherical particles. Clay with high aspect ratio is more efficient in restricting the rubber chains and in resisting the development of cracks than spherical fillers.

The effect of air aging on the mechanical properties of the NR–clay nanocomposite with 10 phr clay is shown in Figure 7. The NR filled with 10 phr carbon black is compared to the NR–clay nanocomposite. As seen in Figure 7, tensile strength and elongation at break for both the NR–clay nanocomposite and the NR filled with carbon black decrease with the increase in aging time. Nonetheless, after 7 days of aging, the tensile strength and elongation at break of the NR–clay nanocomposite are 14.7 MPa and 452%, much higher than 9.0 MPa and 388% for the NR filled with carbon black. It can be seen that NR–clay nanocomposites exhibit better antiaging properties than the NR filled with carbon black with prolonged aging, which may originate from the fact that the NR–clay nanocomposite has the excellent gas barrier property discussed later.

The gas permeability of gum NR vulcanizate and NR–clay nanocomposites is presented in Table IV. As shown in Table IV, the nitrogen permeability reduces with an increased amount of clay. Compared with the gum NR vulcanizate, the nitrogen permeability of NR–clay nanocomposites with 5, 10, 20, 30, and 40 phr clay reduces by 24.8, 34.6, 46.5, 54.0, and 64.1%, respectively. It can be concluded that the clay layers with the large aspect ratio and the planar orientation lead to the great increase of the diffusion distance by creating a tortuous path for the diffusing gas[17,18].

Properties of CR–clay nanocomposites

Like NR, CR is also strain-induced crystallization. CR–clay nanocomposites are prepared by the same method and the mechanical properties are presented in Table V. CR–clay nanocomposites exhibit the highest hardness, modulus, and tear strength among the

TABLE IV
Nitrogen Permeabilities of NR–Clay Nanocomposites(10^{-17} m^2/pa · s)

Clay content, phr	0	5	10	20	30	40
Permeability	13.70 ± 0.2	10.30 ± 0.2	8.96 ± 0.2	7.33 ± 0.2	6.30 ± 0.2	4.92 ± 0.2

TABLE V
Mechanical Properties of CR–Clay Nanocomposites

Properties	Loading of fillers/phr	0	5	10	20	30
Hardness, Shore A	Nano-clay	43	52	64	78	82
	N330	—	—	50	58	64
	Silica	—	—	48	66	68
Modulus at 300%, MPa	Nano-clay	1.29	3.9	7.2	13.1	13.2
	N330	—	—	3.1	5.8	10.0
	Silica	—	—	2.0	3.5	4.1
Tensile strength, MPa	Nano-clay	23.5	25	20.7	14.1	13.4
	N330	—	23.6	25.0	25.1	26.5
	Silica	—	21.0	21.7	20.5	19.0
Tear strength, ($KN \cdot m^{-1}$)	Nano-clay	24.6	58.9	—	72.3	76.4
	N330	—	—	51.6	57.5	65.9
	Silica	—	—	37.3	45.0	69.4

three composites, which is similar to those of NR–clay nanocomposites.

CONCLUSIONS

In the NR–clay nanocomposites prepared by cocoagulating the NR latex and clay aqueous suspension, the clay layers are homogeneously dispersed in NR matrix at a nano level, but not exfoliated completely. The presence of nanoclay (more than 10 phr) inhibits the development of crystallization of NR on stretch. Compared with NR filled with conventional filler, NR–clay nanocomposites exhibit excellent mechanical, antiaging, and gas barrier properties. Like NR–clay nanocomposites, CR–clay nanocomposites also exhibit high hardness, modulus, and tear strength. These new materials can be applied in rubber products, such as inner tubes, inner-liners, and dumpers.

References

1. Kojima, Y.; Usuki, A.; Kawasumi, M.; Okada, A.; Kurauchi, T.; Kamigaito, O. J Appl Polym Sci 1993, 49, 1259.
2. Messersmith, P. B.; Giannelis, E. P. J Polym Sci Part A Polym Chem 1995, 33, 1047.
3. Giannelis, E. P. Adv Mater 1996, 8, 29.
4. Gilman, J. W.; Kashiwagi, T. SAMPE J 1997, 33, 40.
5. Vaia, R. A.; Price, G.; Ruth, P. N.; Nguyen, H. T. Lichtenhan, J Appl Clay Sci 1999, 15, 67).
6. Liu, T. M.; Baker, W. E.; Langille, K. B.; Nguyen, D. T.; Bernt, J. O. J Vinyl Additive Technol 1998, 4, 246.
7. Wang, S. J.; Long, C. F.; Wang, X. Y.; Li, Q.; Qi, Z. N. J Appl Polym Sci 1998, 69, 1557.
8. Kojima, Y.; Fukumori, K.; Usuki, A.; Okada, A.; Kurauchi, T.J Mater Sci Lett 11993, 2, 889.
9. Ganter, M.; Gronski, W.; Semke, H.; Zilg, T.; Thomann, C.; Muhlhaupt, R. Kautschuk Gummi Kunstoffe 2001, 54, 166).
10. Moet, A.; Akelah, A.; Salahuddin, N.; Hiltner, A.; Baer, E. Proc Mater Re. Soc San Francisco, April 2, 1994.
11. Zhang, L. Q.; Wang, Y. Z.; Yu, D. S.; Wang, Y. Q.; Sun, Z. H. CN 98 101496.8, 1998.
12. Wu, Y. P.; Zhang, L. Q.; Wang, Y. Q.; Liang, L.; Yu, D. S. J Appl Polym Sci 2001, 82, 2842.
13. Zhang, L. Q.; Wang, Y. Z.; Wang, Y. Q.; Sui, Y.; Yu, D. S. J Appl Polym Sci 2000, 78, 1873.
14. Wang, Y. Z.; Zhang, L. Q.; Tang, C. H.; Yu, D. S. J Appl Polym Sci 2000, 78, 1879.
15. Wu, Y. P.; Zhang, L. Q.; Wang, Y. Z.; Wang, Y. Q.; Sun, Z. H.; Zhang, H. F.; Yu, D. S. Chinese J Mat Res 2000, 14, 188.
16. Ray, S. S.; Okamoto, M. Progr Polym Sci 2003, 28, 1539.
17. Wu; Y. P.; Jia, Q. X.; Zhang, L. Q.; Yu, D. S. J Appl Polym Sci 2003, 89, 385.
18. Zhang, H. F.; Feng, Y. X.; Wang, Y. Q.; et al. China Rubber Ind 2001, 48, 587.